International Conference on Computer Applications in Electrical Engineering Recent Advances, Roorkee, Feb. 21-23, 2002

ROTOR FLUX ORIENTED SENSORLESS INDUCTION MOTOR DRIVE FOR LOW POWER APPLICATIONS

K. B. Mohanty
Electrical Engg. Department,
Regional Engineering College
ROURKELA

A. Routray N. K. De
Electrical Engg. Department,
Indian Institute of Technology
KHARAGPUR

kbmohanty@nitrkl.ac.in, barada5@rediffmail.

Abstract **:** *This paper presents a new rotor flux oriented linearizing control with speed estimation scheme for adjustable speed induction motor (IM) drive. In this scheme, rotor flux oriented vector control is used to linearize the IM drive, and decouple torque and flux. Also, a stator flux based flux estimator is used to estimate the synchronous speed. The motor speed is estimated by measuring only two line currents and two line voltages. A moving average algorithm is used to filter the ripples in the estimated speed. Proportional-cum-Integral controllers are designed for sensorless speed control. Simulation studies show that the sensorless speed control scheme can achieve fast transient response and at the same time maintain a wide speed control range.*

1. INTRODUCTION

Induction motor is very widely used in industry, because of its simple and robust structure, higher torque-to-weight ratio, higher reliability and ability to operate in hazardous environment. But control of induction motor is a challenging task, as its dynamical system is nonlinear, the rotor variables are not measurable, and physical parameters are most often not accurately known. The control of the induction motor has attracted much attention in the last decade. One of the most significant developments in this area has been the field oriented control [1, 2].

In many industry applications it is neither possible nor desirable to implement speed sensors for control of induction motors because inverters can satisfy the speed control requirements, and from the standpoints of cost, size, noise immunity and reliability of the drive. However, these open-loop controlled inverters have their shortcomings, such as slow dynamic response, poor speed regulation, and limited speed control range. So, the development of shaft sensorless adjustable speed drive has become an important research topic [3, 4]. There are two major concerns in the sensorless, field oriented control of induction motor drive. One is the decoupling control scheme and the other one is the rotor speed estimation algorithm. Both are highly dependent on the motor parameters. Rotor flux orientation scheme [2], though more parameter sensitive has certain advantages compared to stator or airgap flux orientation schemes, as complete decoupling of flux and torque is obtained without an additional decoupling network. For low power induction motor drives, where parameter sensitivity is not considerable, rotor flux orientation scheme can be used without parameter estimation technique. Although many speed estimation algorithms and sensorless control schemes [5] have been developed during the past few years, a simple, effective, and low sensitivity sensorless control scheme for low power induction motor drives is a worth pursuing goal.

In the present paper, induction motor model is reviewed in section 2. In section 3, rotor flux oriented linearization scheme is discussed. Section 4 details the sensorless control scheme. Results are discussed in section 5.

2. INDUCTION MOTOR MODEL

From the voltage equations of the induction motor in the arbitrary rotating d-q reference frame, the state space model with stator current and rotor flux components as state variables is:

$$\frac{d}{dt}\begin{bmatrix} i_s \\ \psi_r \end{bmatrix} = \begin{bmatrix} A_{11} & A_{12} \\ A_{21} & A_{22} \end{bmatrix}\begin{bmatrix} i_s \\ \psi_r \end{bmatrix} + \begin{bmatrix} B_1 \\ 0 \end{bmatrix} v_s \qquad (1)$$

where, $i_s = y = \begin{bmatrix} i_{ds} & i_{qs} \end{bmatrix}^T$, $\psi_r = \begin{bmatrix} \psi_{dr} & \psi_{qr} \end{bmatrix}^T$,

$v_s = \begin{bmatrix} v_{ds} & v_{qs} \end{bmatrix}^T$,

$A_{11} = -a_1 I - \omega_e J$, $A_{12} = a_2 I - P a_3 \omega_r J$,

$A_{21} = a_5 I$, $A_{22} = -a_4 I - (\omega_e - P\omega_r) J$,

$B_1 = c I$.

$$I = \begin{bmatrix} 1 & 0 \\ 0 & 1 \end{bmatrix}, \quad \text{and} \quad J = \begin{bmatrix} 0 & -1 \\ 1 & 0 \end{bmatrix}$$

$c = L_r / (L_s L_r - L_m^2)$,

$a_1 = c R_s + c R_r L_m^2 / L_r^2$,

$a_2 = c R_r L_m / L_r^2$,

$a_3 = c L_m / L_r$, $a_4 = R_r / L_r$,

$a_5 = R_r L_m / L_r$

The torque developed by the motor is:

$$T_e = K_t \, (\psi_{dr} \, i_{qs} - \psi_{qr} \, i_{ds}) \tag{2}$$

where, torque constant, $K_t = 3 \, P \, L_m \, / 2 \, L_r$

3. LINEARIZATION USING ROTOR FLUX ORIENTATION

The conditions required for decoupling control [6] are:

$$\psi_{qr} = 0 \quad \text{and} \quad \dot{\psi}_{qr} = 0 \tag{3}$$

From (1), decoupling is obtained, when

$$\omega_{sl} = \frac{R_r \, L_m}{L_r} \cdot \frac{i_{qs}}{\psi_{dr}} \tag{4}$$

When (3) is satisfied, the dynamic behavior of the induction motor is:

$$\dot{i}_{ds} = - a_1 \, i_{ds} + a_2 \psi_{dr} + \omega_e \, i_{qs} + c \, v_{ds} \tag{5}$$

$$\dot{i}_{qs} = - \omega_e \, i_{ds} - a_1 \, i_{qs} - P \, a_3 \, \omega_r \, \psi_{dr} + c \, v_{qs} \tag{6}$$

$$\dot{\psi}_{dr} = - a_4 \, \psi_{dr} + a_5 \, i_{ds} \tag{7}$$

$$T_e = K_t \, \psi_{dr} \, i_{qs} \tag{8}$$

Even in the induction motor model described by Eq. (5-8), nonlinearity and interaction exist. The transition from field oriented voltage components, v_{ds} and v_{qs} to current components as in (5) and (6), involves leakage time constants and interactions. As the developed torque is a product of ψ_{dr} and i_{qs}, the overall system remains coupled. The interaction between current components, and nonlinearity in the overall system are eliminated by using a nonlinear control approach [7, 8]. This approach consists of change of coordinates and use of nonlinear inputs to linearize the system equations.

Nonlinear control inputs of the form, u_1 and u_2 are used to linearize Eq. (5-8) as described in [8]. The input voltages, v_{ds} and v_{qs} to the motor in terms of u_1 and u_2 are given by:

$$v_{ds} = \frac{1}{c}(-\omega_e i_{qs} + u_1) \tag{9}$$

$$v_{qs} = \frac{1}{c}\left[P\omega_r (i_{ds} + a_3 \psi_{dr}) + \frac{u_2}{K_t \psi_{dr}} \right] \tag{10}$$

The induction motor system with these new inputs, is decoupled into two linear subsystems: (*i*) Electrical, and (*ii*) Mechanical, described by the following equations.

Electrical subsystem:

$$\dot{i}_{ds} = -a_1 i_{ds} + a_2 \psi_{dr} + u_1 \tag{11}$$

Mechanical subsystem:

$$\dot{T}_e = -(a_1 + a_4) T_e + u_2 \tag{12}$$

4. SENSORLESS CONTROL SCHEME

The block diagram of the sensorless speed control scheme is shown in Fig. 1. This sensorless speed control system consists of three major parts: (A) P-I controllers for speed and current, (B) flux-weakening controller, (C) speed estimator.

(A) P-I Controllers for speed and current

The performance of a drive system largely depends upon the choice of the controller. P-I controller is time tested for its transient and steady state performances, and theory is well established for its design. One P-I controller is used for the flux, or flux component of current as it is adequate for good dynamic response. One P-I controller is used for the speed control, and another for the torque, or torque component of current. The reason for using two P-I controllers (one for speed and the other for torque) in a nested fashion is the significant difference in the time constants of the speed and current, or the electromagnetic torque. The design procedure for these P-I controllers are detailed in [8]. The gains are:

$K_{pd} = 151.24$, $K_{id} = 43640$, $K_{pw} = 0.26$, $K_{iw} = 1.98$, $K_{pq} = 100$, $K_{iq} = 29877$.

(B) Flux weakening controller

The flux weakening controller is used to regulate the magnitude of rotor flux linkage command ψ^*_{dr} such that the motor will operate in constant torque mode when motor speed is below base speed and in constant power mode when motor speed is above the base speed. The flux weakening control algorithm is as follows.

$$\psi^*_{dr} = \begin{cases} \psi_R & \text{if } \hat{\omega}_r \le \omega_b \\ \psi_R \, \dfrac{\omega_b}{\hat{\omega}_r} & \text{if } \hat{\omega}_r \ge \omega_b \end{cases} \tag{13}$$

where, ψ_R = rated rotor flux linkage in V· s

ω_b = base speed in rad/s

The rotor flux command is then converted to an equivalent field current command in the rotating reference frame.

(C) Speed estimator

The rotor speed is estimated by estimating either synchronous, or slip speed, assuming the other to be known. In the speed estimation scheme described in this paper, the synchronous speed is estimated and the slip speed is assumed to be command value. So, the estimated rotor speed is given by:

$$\hat{\omega}_r = \frac{\hat{\omega}_e - \omega^*_{sl}}{P} \tag{14}$$

The synchronous speed is estimated from the rotor flux model, or the stator flux model. The principle of both the methods are briefly explained below.

If $\psi_{\beta r}$ and $\psi_{\alpha r}$ are the two components of the *rotor flux vector* in the stationary $(\alpha-\beta)$ reference frame, the electrical angle of the rotor flux vector is defined as:

$$\theta_{\psi_r} = \tan^{-1}\left(\frac{\psi_{\beta r}}{\psi_{\alpha r}}\right) \tag{15}$$

The derivative of this rotor flux angle (with respect to time) gives the instantaneous electrical synchronous speed.

$$\omega_e = \dot{\theta}_{\psi_r} = \frac{\psi_{\alpha r}\,\dot{\psi}_{\beta r} - \psi_{\beta r}\,\dot{\psi}_{\alpha r}}{\psi_{\alpha r}^2 + \psi_{\beta r}^2} \tag{16}$$

If $\psi_{\alpha s}$ and $\psi_{\beta s}$ are the two components of the *stator flux vector* in the stationary $(\alpha-\beta)$ reference frame, the electrical angle of the stator flux vector is defined as:

$$\theta_{\psi_s} = \tan^{-1}\left(\frac{\psi_{\beta s}}{\psi_{\alpha s}}\right) \tag{17}$$

The derivative of this stator flux angle (with respect to time) gives the instantaneous electrical synchronous speed.

$$\omega_e = \dot{\theta}_{\psi_s} = \frac{\psi_{\alpha s}\,\dot{\psi}_{\beta s} - \psi_{\beta s}\,\dot{\psi}_{\alpha s}}{\psi_{\alpha s}^2 + \psi_{\beta s}^2} \tag{18}$$

From the voltage equations of the induction motor in the stationary $(\alpha-\beta)$ reference frame [9], the stator and rotor flux linkages are given by

$$\begin{aligned}\psi_{\alpha s} &= \int_0^t (v_{\alpha s} - R_s\, i_{\alpha s})\, dt \\ \psi_{\beta s} &= \int_0^t (v_{\beta s} - R_s\, i_{\beta s})\, dt\end{aligned} \tag{19}$$

$$\begin{aligned}\psi_{\alpha r} &= \frac{L_r}{L_m}(\psi_{\alpha s} - \sigma L_s\, i_{\alpha s}) \\ \psi_{\beta r} &= \frac{L_r}{L_m}(\psi_{\beta s} - \sigma L_s\, i_{\beta s})\end{aligned} \tag{20}$$

Eq. (19) shows that the stator flux depends on the stator resistance and measured stator voltages and currents. Eq. (20) shows that the rotor flux depends on the estimated stator flux, and requires the knowledge of the inductances of the machine, especially the stator leakage inductance (σL_s). Usually, the stator resistance can be measured with fair accuracy. Hence, stator flux can be estimated more accurately as compared to the rotor flux. Therefore, estimated stator flux is used to derive the synchronous frequency from (18).

The current components in the stationary $(\alpha-\beta)$ reference frame are calculated from the measured phase currents i_b and i_c.

$$i_{\beta s} = \frac{2}{3}\left(i_a - \frac{1}{2} i_b - \frac{1}{2} i_c\right) = -(i_b + i_c) \tag{21}$$

$$i_{\alpha s} = \frac{2}{3}(i_c - i_b)\cdot\frac{\sqrt{3}}{2} = \frac{1}{\sqrt{3}}(i_c - i_b) \tag{22}$$

Similarly the voltage components in the stationary $(\alpha-\beta)$ reference frame are calculated from the measured line voltages v_{ab} and v_{ac}.

$$v_{\beta s} = \frac{2}{3}\left(v_a - \frac{1}{2} v_b - \frac{1}{2} v_c\right) = \frac{1}{3}(v_{ab} + v_{ac}) \tag{23}$$

$$v_{\alpha s} = \frac{2}{3}(v_c - v_b)\cdot\frac{\sqrt{3}}{2} = \frac{1}{\sqrt{3}}(v_{ab} - v_{ac}) \tag{24}$$

After the stationary $(\alpha-\beta)$ reference frame components of measured voltages and currents are obtained by (21-24) in every sampling interval, the derivatives of the stator flux components are obtained in the discrete domain, using (19) as follows.

$$\begin{aligned}\dot{\psi}_{\alpha s}(k) &= v_{\alpha s}(k) - R_s\, i_{\alpha s}(k) \\ \dot{\psi}_{\beta s}(k) &= v_{\beta s}(k) - R_s\, i_{\beta s}(k)\end{aligned} \tag{25}$$

The stator flux components are then obtained from their derivatives as follows.

$$\begin{aligned}\psi_{\alpha s}(k) &= \psi_{\alpha s}(k-1) + \dot{\psi}_{\alpha s}(k)\, T_s \\ \psi_{\beta s}(k) &= \psi_{\beta s}(k-1) + \dot{\psi}_{\beta s}(k)\, T_s\end{aligned} \tag{26}$$

where, T_s is the sampling time.

Then, the estimated synchronous frequency is obtained from (18) as:

$$\hat{\omega}_e(k) = \frac{\psi_{\alpha s}(k)\,\dot{\psi}_{\beta s}(k) - \psi_{\beta s}(k)\,\dot{\psi}_{\alpha s}(k)}{\psi_{\alpha s}^2(k) + \psi_{\beta s}^2(k)} \tag{27}$$

The estimated rotor speed is obtained by substituting (27) in (14), and using the command value of slip speed, ω_{sl}^* required for decoupling, as given by (4).

$$\omega_{sl}^*(k) = \frac{R_r\, L_m}{L_r}\cdot\frac{i_{qs}^*(k)}{\psi_{dr}^*(k)} \tag{28}$$

where, command value of flux linkage, $\psi_{dr}^*(k)$ is given by (13), and command value of torque component of current (q-axis stator current) is given by

$$i_{qs}^*(k) = \frac{T_e^*(k)}{\frac{3}{2} P \frac{L_m}{L_r}\psi_{dr}^*(k)} \tag{29}$$

$T_e^*(k)$ = reference torque in N·m, generated from the speed error, through the speed controller.

In the calculation of the rotor angular speed, the sampling time is set at the same value (T_s) as used in the current control loop, to obtain a fast dynamic response. However, in this way the estimated speed is also corrupted by the current ripples. In practical conditions, the time constant of current loop is much smaller than that of the speed loop. In other words, the current loop bandwidth is much wider than the speed loop bandwidth. Therefore, a moving average algorithm is used to smooth the estimated speed.

The formula used is:

$$\hat{\omega}_r(n) = \frac{1}{N}\sum_{k=1}^{N}\hat{\omega}_r(n-k) \qquad (30)$$

where,

$$N = T_2 / T_1$$

T_1 = sampling time of the current control loop
T_2 = sampling time of the speed control loop

5. RESULTS AND DISCUSSIONS

The simulation study of the drive system has been carried out, when the rotor speed is estimated and the estimated speed used in the rotor flux oriented linearizing control algorithm. The 3-phase induction motor used in the simulation study has the following rating and parameters: 0.75 kW, 220V, 3A, 50 Hz, 1440 rpm, R_s = 6.37 ohms, R_r = 4.3 ohms, L_s = L_r = 0.26 H, L_m = 0.24 H, J = 0.0088 Kg m^2, β = 0.003 N m s/rad. The simulation result is presented in Fig. 2, for a step change in speed command from 1000 r/min to 1300 r/min. The speed response exhibits an overshoot of 200 r/min and 3% settling time of 0.32 s. The estimated speed response is similar to the actual speed response, except the fact that it contains ripple of peak-to-peak value, 50 r/min (1.36% rms) about the steady state value. The d-axis stator current exhibits overshoot up to 2.2 A and oscillation for 0.3 s. The q-axis stator current exhibits overshoot up to 6.5 A and oscillation for 0.8 s. Peak phase current of stator increases from 2 A to 6.7 A and exhibits oscillation for 0.3 s during the transient period. It can be stated that ripple in the estimated speed may be reduced by increasing the sample time (T_2 in Eq. (30)) in the speed estimation.

6. CONCLUSIONS

The successful implementation of sensorless induction motor (IM) drive depends on not only fast and accurate rotor speed estimation, but also requires a well tuned decoupling control of the induction motor. In sensorless IM drive, speed estimation and decoupling control are always coupled together. Both are dependent on the knowledge of related motor parameters. A slightly detuned IM drive under closed loop speed control can still achieve good speed regulation due to real speed feedback. However, a detuned sensorless drive will result in inferior transient and steady state responses, and may lead to system instability. This situation gets worsened especially when operating in the low speed range. So, speed estimation with low sensitivity to motor parameter variations is very important. The presented sensorless speed control scheme employs rotor flux oriented linearizing control to achieve linearization and decoupling. Stator flux based flux estimator is used to estimate the speed. Studies show that this scheme is especially suitable for small size induction motors with known rotor time constant.

NOMENCLATURE

P: number of pole pairs,

ω_{sl}^{*} : command slip speed (electrical)

$\hat{\omega}_r$: estimated rotor angular (mechanical) speed

$\hat{\omega}_e$: estimated synchronous speed (electrical),

* : superscript denoting reference or command

σ : leakage coefficient = $(1 - L_m^2 / L_s L_r)$

K_{pd}, K_{id}: P-I gains of d-axis current controller,
K_{pw}, K_{iw}: P-I gains of speed controller,
K_{pq}, K_{iq}: P-I gains of q-axis current controller

REFERENCES

[1] F. Blaschke, "The principle of field orientation as applied to the new TRANSVEKTOR closed-loop system for rotating-field machines," Siemens Review, vol.39, no.5, May 1970, pp.217-220.

[2] W. Leonhard, *Control of Electrical Drives*, 2nd ed., Berlin, Germany: Springer-Verlag, 1990.

[3] K. Ohnishi, N. Matsui, and Y. Hori, "Estimation, identification and sensorless control in motion control system," Proc. of IEEE, vol. 82, no. 8, Aug. 1994, pp. 1253-1265.

[4] J. Holtz, "Speed estimation and sensorless control of AC drives," IEEE IECON Conf. Rec., vol. 2, 1993, pp. 649-654.

[5] K. Rajashekara, A. Kawamura, and K. Matsuse, *Sensorless Control of AC Motor Drives*, Piscataway, NJ, IEEE Press, 1996.

[6] B. K. Bose, *Power Electronics and AC Drives,* Englewood Cliffs, NJ: 1986.

[7] J. J. E. Slotine and W. Li, *Applied Nonlinear Control*, NJ: Prentice Hall International, Englewood Cliffs, 1991.

[8] K. B. Mohanty and N. K. De, "Nonlinear controller for induction motor drive," Proc. of IEEE International Conference on Industrial Technology (ICIT), 2000, Goa, India, pp. 382-387.

[9] P. C. Krause, *Analysis of Electric Machinery*, McGraw-Hill, New York, 1986

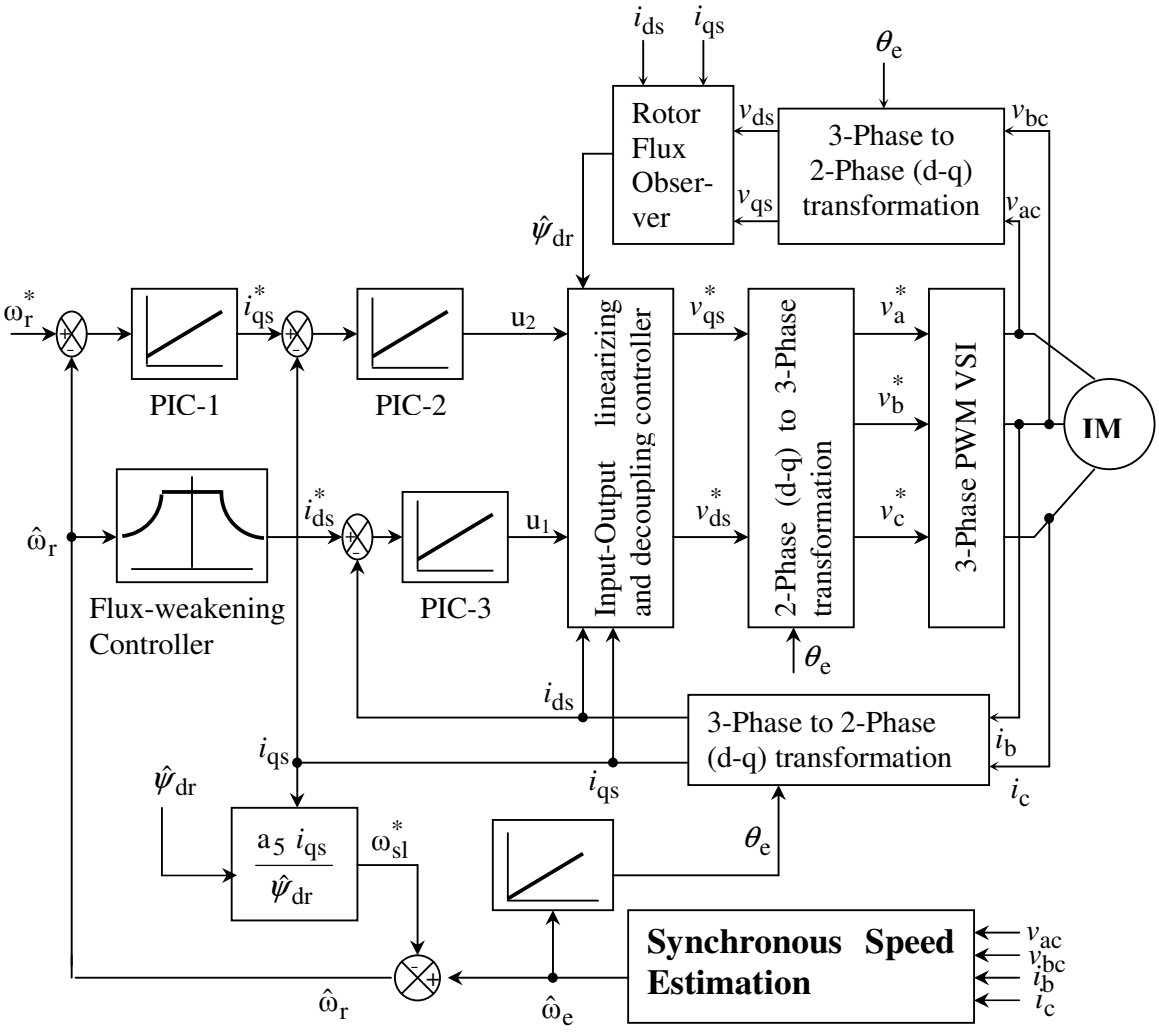

Fig. 1 Block diagram of sensorless speed control scheme

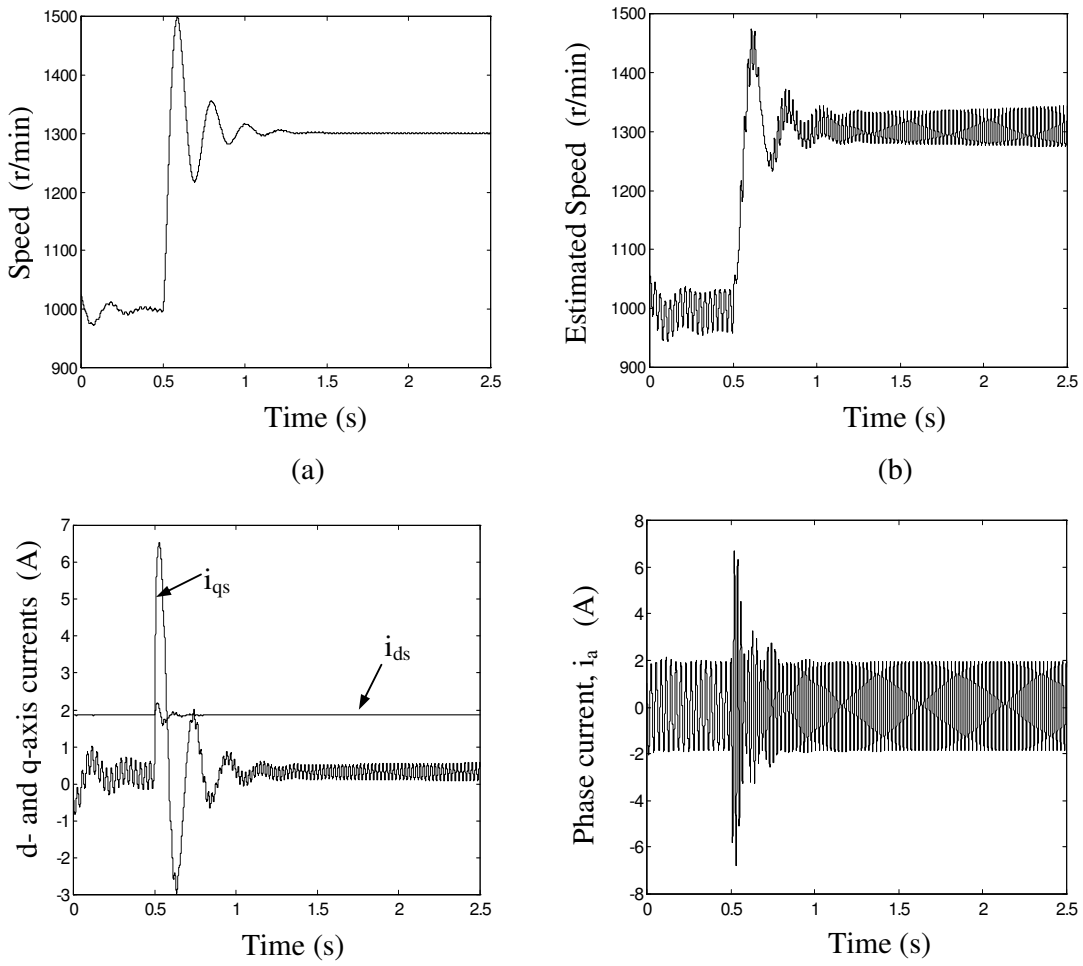

Fig. 2 Simulation response for step change in speed with speed estimation:
(a) Speed, (b) Estimated speed, (c) d- and q-axis stator currents, (d) Stator phase current,